Dynamics of grain boundary motion coupled to shear deformation: An analytical model and its verification by molecular dynamics

V. A. Ivanov* and Y. Mishin†

Department of Physics and Astronomy, George Mason University, MSN 3F3, 4400 University Drive, Fairfax, Virginia 22030, USA

(Received 4 February 2008; revised manuscript received 25 June 2008; published 11 August 2008)

Many atomically ordered grain boundaries (GBs) couple to applied mechanical stresses and are moved by them, producing shear deformation of the lattice they traverse. This process does not require atomic diffusion and can be implemented at low temperatures by deformation and rotation of structural units. This so-called coupled GB motion occurs by increments and can exhibit dynamics similar to the stick-slip behavior known in atomic friction. We explore possible dynamic regimes of coupled GB motion by two methods. First, we analyze a simple one-dimensional model in which the GB is mimicked by a particle attached to an elastic rod and dragged through a periodic potential. Second, we apply molecular dynamics (MD) with an embedded-atom potential for Al to simulate coupled motion of a particular tilt GB at different temperatures and velocities. The stress-velocity-temperature relationships established by both methods are qualitatively similar and indicate highly nonlinear dynamics at low temperatures and/or large velocities. At high temperatures and/or slow velocities, the character of the GB motion changes from stick slip to driven random walk and the stress-velocity relation becomes approximately linear. The MD simulations also reveal multiple GB jumps due to dynamic correlations at high velocities, and a transition from coupling to sliding at high temperatures.

DOI: 10.1103/PhysRevB.78.064106 PACS number(s): 61.72.Bb, 61.72.Mm, 68.35.Af

I. INTRODUCTION

Many grain boundaries (GBs) have the property that their normal motion requires a simultaneous relative translation of the adjacent grains parallel to the GB plane.[1–4] Conversely, any relative translation of the grains causes a normal displacement of the boundary. Such GBs are said to be *coupled* and their response to applied driving forces can be different from that of uncoupled GBs. Specifically, if a shear stress is applied parallel to a coupled GB, it creates a driving force for its normal motion.[5] This motion, in turn, produces shear deformation of the material swept by the boundary. Conversely, if a coupled GB is driven by capillary forces or a volume driving force due to elastic or magnetic anisotropy, the boundary shears the lattice region it traverses and produces a rigid translation of the grains. It can be shown that coupled motion of a curved GB induces grain rotation and vice versa.[1,6] The coupling effect is characterized by a factor β equal to the ratio of the tangential grain translation velocity v to the accompanying normal GB displacement velocity v_n. The coupling is called perfect if β is a geometric constant that depends only on the GB crystallography but not on the GB velocity, driving force or any other physical parameters.

The coupled GB motion is a rather common effect. Atomistic computer simulations have revealed dozens of coupled GBs.[2–4,6] Stress-induced GB motion has been observed in experiments on bicrystals in both metals[7–12] and ceramic materials.[13] The experimental coupling factors were found[7,8] to match the perfect values predicted by the geometric theory.[2–4] It is believed that the coupling effect might be responsible for the stress-driven GB motion and stress-induced grain growth in nanocrystalline materials.[14–16]

Among the unsolved problems and future work directions outlined in Ref. 4, it was pointed out that coupled GB motion can exhibit a rich variety of dynamics that need to be identified and understood. In particular, it was suggested that the stress-velocity relation can change significantly as the stop-and-go (stick-slip) character of motion observed at low temperatures[3,4] transforms to driven random walk at high temperatures. The stress-velocity relation in the stick-slip regime was recently studied by accelerated molecular dynamics (MD) over a wide velocity range[17] at one fixed temperature. The temperature dependence of GB dynamics was not examined in that work.

In this paper we continue to investigate the dynamics of coupled GB motion, now focusing on its temperature dependence. We apply two different approaches to the problem: First, we analyze a one-dimensional analytical model of coupling which, despite its simplistic character, permits a derivation of useful stress-velocity relations that can be tested against atomistic simulations. Second, we conduct MD simulations of stress-driven and spontaneous coupled motion of a particular GB over a wide temperature range and reveal the transition from the stick-slip regime to Brownian dynamics. This combination of the analytical and MD approaches is the central point of this paper.

While the previous MD simulations[2–4,17] employed copper as a model material, in this work we switch to aluminum GBs in order to be more compatible with recent[7,8] and ongoing[18] experiments on Al bicrystals. This also guarantees a seamless connection to our current work focusing on crystallographic aspects of coupling in Al boundaries. We emphasize, however, that most of our results are generic and should not be dependent on the material.

In this paper we treat coupled GB motion as motion through a periodic energy landscape. To explain the origin of this landscape, consider an example of a planar tilt boundary in a pure metal at zero temperature. Assume for simplicity that the tilt angle θ is such that a coincident site lattice (CSL)[19] arises and the GB lies in a CSL plane. Such boundaries typically have a periodic structure consisting of polyhedral structural units.[19] Due to translational symmetry of

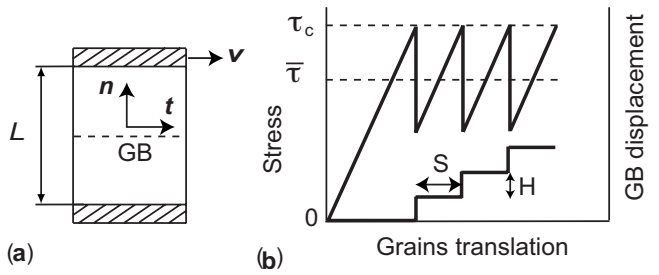

FIG. 1. (a) A gedanken experiment in which a GB (shown as a dashed line) is moved by a shear stress. The tilt axis of the GB is normal to the viewer, **n** is a unit vector normal to the GB plane, and **t** is a unit vector normal to both **n** and the tilt axis. The dashed areas designate two slabs used as clamps. The stress is applied by moving the upper slab with a fixed velocity **v** parallel to **t** while the lower slab remains fixed. L is the normal size of the dynamic region, which plays the role similar to the grain size. (b) If the coupling is perfect, the GB moves by increments of H accompanied by relative grain translations S. The stress exhibits a saw-tooth behavior with a peak value τ_c and an average $\bar{\tau}$.

the bicrystal, there is an infinite number of GBs that have exactly the same energy and identical atomic structures obtainable from one another by rigid translations. All these GBs are parallel to each other and only differ in the translational state of the grains.

Energetically, these equivalent GBs correspond to potential energy minima in the $3N$-dimensional configuration space of the bicrystal, with N being the number of atoms in the system. The GB motion can be coupled if the boundary structure permits translations between neighboring equivalent positions by relatively small atomic displacements without atomic diffusion. These displacements can usually be described as deformations and rotations of the structural units and require overcoming a certain energy barrier E_0. If a driving force is applied and the GB is set to motion, it moves by jumping between the equilibrium positions. The critical stresses required for this process can depend on temperature and the GB velocity. Investigating these relations is the goal of this paper.

II. DYNAMICS OF COUPLED BOUNDARY MOTION

In this section we outline some problems related to dynamics of coupled GB motion. We will consider a particular coupling mode, in which neighboring GB positions are a distance H apart while the coupled grain translations are by S in a direction **t** normal to the tilt axis [Fig. 1(a)]. The perfect coupling factor in this mode is $\beta=S/H$.

A. Zero-temperature dynamics

At 0 K and in the absence of applied stresses, the GB is initially in a particular equilibrium position. Suppose a shear stress is applied to the bicrystal by holding the lower grain and moving the upper grain with a constant velocity **v** parallel to **t** [Fig. 1(a)]. The force acting on the upper grain is transmitted through the lattice regions and creates a local stress $\hat{\boldsymbol{\sigma}}$ at the GB. This stress elastically deforms the GB structural units and reduces the energy barrier for the GB displacement to a new position, simultaneously raising the barrier in the opposite direction.

We are particularly interested in the shear stress $\tau=(\hat{\boldsymbol{\sigma}}\cdot\mathbf{n})\cdot\mathbf{t}$ resolved in the direction of the grain translation. When τ reaches a critical value τ_c^0,[20] the stress-reduced barrier E turns to zero. The GB becomes mechanically unstable and jumps to a new position. The accompanying grain translation produces a permanent shear deformation of the bicrystal and the stress drops. As the upper grain continues to move, the stress builds up again until it reaches τ_c^0 and the GB makes another step. As this process continues, the GB moves forward by increments of H while the stress τ displays a saw-tooth behavior as indicated in Fig. 1(b).[21] This incremental motion, in which the GB is trapped in one energy minimum until it loses stability and jumps to a new minimum, can be classified as a stick-slip process by analogy with other similar phenomena.[22–25]

Between the increments of the GB motion, the stress increases as a linear function of time assuming linear elasticity. The magnitude of the stress drop at each step is then proportional the increment of the shear deformation, S/L, and thus inversely proportional to the system size L in the normal direction. It follows that the stress $\bar{\tau}^0$ averaged over a cycle of this process is

$$\bar{\tau}^0 = \tau_c^0 - KS/2L, \tag{1}$$

where K is the appropriate elastic modulus. If L increases, the stress drop decreases and in the limit of $L\to\infty$ the GB moves under a nearly constant stress. In the other limit, when the grains are small, the stress drops to a small value and can even become negative.[4] In the latter case, the stress arising immediately after a jump is driving the GB back to the previous position. Importantly, the value of the peak stress should be insensitive to L since this value depends only on the GB structure and the coupling mode. These predictions regarding the grain-size dependence of the stress behavior need to be tested by atomistic simulations.

B. Finite temperature dynamics

At finite temperatures, thermal fluctuations assist the GB in overcoming the barrier and it can jump to a new position when E is still positive, i.e., before the stress reaches τ_c^0. This effectively reduces the critical stress required for the GB motion, making it $\tau_c<\tau_c^0$. By contrast to τ_c^0, the reduced critical stress τ_c is a stochastic quantity that should be characterized by its average and a statistical distribution around it. This stress is anticipated to decrease with temperature as thermal fluctuations intensify. At a fixed temperature, τ_c should increase with v since higher velocities give the GB less time to overcome the barrier before it vanishes. Understanding such relationships among the velocity, stress, and temperature is an important task of GB dynamics. Some of these relations will be investigated later in this paper.

At high temperatures, there is a finite probability for the GB to make a spontaneous jump back to the previous position. We expect that such backward jumps, which should become more frequent as temperature increases, should

eventually destroy the saw-tooth behavior of the stress and replace it by random noise with some average $\bar{\tau}$. In this regime, the critical stress loses its physical significance while $\bar{\tau}$ becomes the most meaningful measure of the stress driving the boundary motion. Reducing the GB velocity at a fixed temperature should produce a similar effect by giving the GB more time to sample both forward and backward jumps according to their probabilities. In fact, if v tends to zero at a high temperature, the forward and backward jumps become equally probable, resulting in a random walk of the boundary between its equilibrium positions.[2,4] In this limit $\bar{\tau}$ must turn to zero by symmetry. If coupled GB motion at small velocities can be treated as a driven Brownian process, one should expect a linear relation between v and $\bar{\tau}$. This prediction[4] seems to be consistent with recent experiments[7,12] but was never verified by computer simulations.

III. ONE-DIMENSIONAL MODEL OF BOUNDARY DYNAMICS

Before we explore some of the regimes of coupled GB motion by atomistic simulations, it is useful to examine a simple one-dimensional model that predicts some important relations between the key dynamic parameters. In a recent paper,[17] a simple mechanical analog of coupled GB motion has been proposed in which the GB is represented by a particle attached to an elastic rod. The particle is dragged through a spatially periodic potential $U(x)$ by pulling the other end of the rod in a direction x. The rod models the elastically deformed grains while $U(x)$ mimics the potential energy landscape of the GB in the absence of applied stresses. The mass m of the particle represents the effective mass of the moving grains while the particle friction against the potential surface and the energy dissipation in the rod capture the damping processes at the GB and inside the grains, respectively. This simple one-dimensional model is rich enough to capture a number of dynamic regimes whose detailed analysis is deferred to a separate publication. Here, we will limit the analysis to a few particular cases and derive analytical expressions that will later be compared with atomistic simulations.

Following Refs. 26 and 27, we describe $U(x)$ by a cosine with a period a (Fig. 2):

$$U(x) = \frac{E_0}{2}\left[1 - \cos\left(\frac{2\pi x}{a}\right)\right]. \tag{2}$$

The minima of $U(x)$ define equilibrium locations of the particle, which are separated by the energy barrier E_0.

Suppose the particle is initially at $x=0$ and the elastic rod begins to exert a force τ on it, pulling the particle to the right. We approximate the modified potential energy around the particle by the tilted cosine $U(x)-\tau x$. This approximation is valid if the rod is soft enough that $2a \ll \tau/k$, where k is the spring constant of the rod (otherwise there is a non-negligible change of τ between the right and left maxima around $x=0$). This tilt of the potential energy reduces the barrier E_+ for the forward jump (to the right) and raises the barrier E_- for the backward jump (to the left). It also shifts the equilibrium point of the particle.

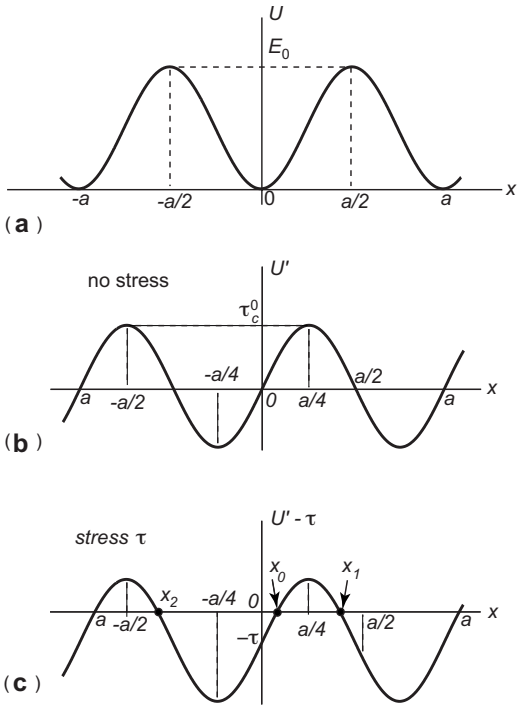

FIG. 2. (a) The potential energy $U(x)$, (b) its derivative $U'(x)$ and (c) the total force $U'(x)-\tau$ (c) in the one-dimensional model of coupling.

The new maxima and minima of the potential energy satisfy the condition $U'(x)-\tau=0$, i.e.,

$$\tau_c^0 \sin\left(\frac{2\pi x}{a}\right) - \tau = 0, \tag{3}$$

where we denote $\tau_c^0 \equiv \pi E_0/a$ (Fig. 2). From this equation, the new equilibrium position is

$$x_0 = \frac{a}{2\pi}\arcsin\left(\frac{\tau}{\tau_c^0}\right), \tag{4}$$

and the maxima are at $x_1 = a/2 - x_0$ and $x_2 = -a/2 - x_0$. The energy barriers are found as work done when moving the particle from x_0 to x_1 and x_2, respectively:

$$E_+ = \int_{x_0}^{x_1} [U'(x) - \tau]dx = E_0\left[\sqrt{1-\left(\frac{\tau}{\tau_c^0}\right)^2} - \frac{\pi\tau}{2\tau_c^0}\left(1 - \frac{2}{\pi}\arcsin\frac{\tau}{\tau_c^0}\right)\right], \tag{5}$$

$$E_- = \int_{x_0}^{x_2} [U'(x) - \tau]dx = E_0\left[\sqrt{1-\left(\frac{\tau}{\tau_c^0}\right)^2} + \frac{\pi\tau}{2\tau_c^0}\left(1 + \frac{2}{\pi}\arcsin\frac{\tau}{\tau_c^0}\right)\right]. \tag{6}$$

Consider limiting cases of these expressions. When τ reaches τ_c^0, the barrier E_+ turns to zero while $x_1 \to x_0 \to a/4$. The equilibrium becomes unstable and the particle is bound to make a jump forward. This reveals the meaning of τ_c^0 as

the critical force for the particle motion through the potential landscape at zero temperature. When $\tau=\tau_c^0$, the barrier of the backward jump is $E_-=\pi E_0$. Thus, the "athermal" motion of the particle that starts at $\tau=\tau_c^0$ occurs by forward jumps only.

To determine exactly how E_+ tends zero and E_- to πE_0 when $\tau\to\tau_c^0$, we expand Eqs. (5) and (6) in powers of the small parameter $\sqrt{1-\tau/\tau_c^0}$ and keep only leading terms, obtaining

$$E_+ \approx \sqrt{2}E_0\left(1-\frac{\tau}{\tau_c^0}\right)^{3/2}, \tag{7}$$

$$E_- \approx \pi E_0 \frac{\tau}{\tau_c}. \tag{8}$$

Thus, the barrier E_+ vanishes as $(\tau_c^0-\tau)^{3/2}$, not as $\tau_c^0-\tau$ as one could expect.[28]

In the other limit, when $\tau \ll \tau_c^0$, Eqs. (5) and (6) give

$$E_\pm \approx E_0\left(1 \mp \frac{\pi\tau}{2\tau_c^0}\right), \tag{9}$$

indicating that a small force shifts the forward and backward jump barriers in opposite directions by the same amount proportional to τ.

At a finite temperature T, the particle can make jumps over the barriers by thermal fluctuations. Applying the transition-state theory, the rates of the forward and backward jumps (number of jumps per unit time) are $W_+ = \nu \exp(-E_+/k_BT)$ and $W_- = \nu \exp(-E_-/k_BT)$, respectively. Here, ν is a jump attempt frequency and k_B the Boltzmann factor. The average velocity of the particle is $\bar{v}=a(W_+-W_-)$.

In the small-force limit ($\tau \ll \tau_c^0$), we can apply Eq. (9) to obtain

$$\bar{v} = 2a\nu \exp\left(-\frac{E_0}{k_BT}\right)\sinh\left(\frac{E_0\pi\tau}{2k_BT\tau_c^0}\right). \tag{10}$$

Expanding the hyperbolic sine to the first order in τ leads to the linear force-velocity relation

$$\bar{v} \approx M(T)\tau, \tag{11}$$

where the $M(T)$ needs not to be detailed for this discussion. This linear relation is valid if

$$\frac{E_0\pi\tau}{2k_BT\tau_c^0} \ll 1, \tag{12}$$

i.e., when either the driving force is small or the temperature is high. This regime is best described as driven random walk, or driven Brownian motion.

In the limit of $\tau\to\tau_c^0$, we have $W_+ \gg W_-$ and backward jumps can be neglected. Then,[29–31]

$$\bar{v} \approx aW_+ \approx v_0 \exp\left[-\frac{\sqrt{2}E_0\left(1-\frac{\tau}{\tau_c^0}\right)^{3/2}}{k_BT}\right], \tag{13}$$

where $v_0=\nu a$.

We emphasize that the force-velocity relations obtained are only valid as long as the assumptions of the transition-state theory are satisfied. In particular, after each jump the particle must have enough time to come to thermal equilibrium with the environment before the next jump may occur. This assumption can be violated if the average velocity is too high and/or the energy dissipation processes are too slow.

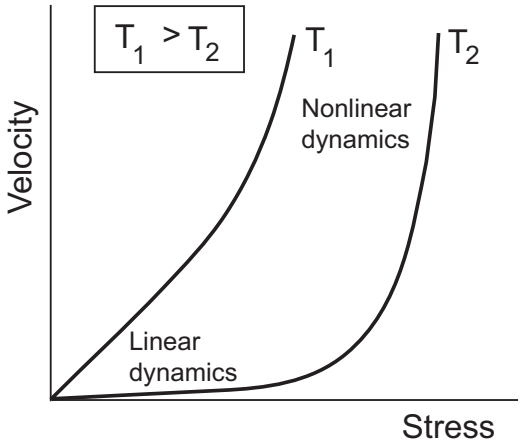

FIG. 3. Velocity-stress relations at high (T_1) and low (T_2) temperatures predicted by the one-dimensional model of coupled GB motion. The regions of the linear dynamics (mobility regime) and nonlinear (exponential) dynamics are indicated.

Translating this analysis from an abstract particle to a moving GB, the force τ should be referred to a unit GB area and becomes the applied shear stress. The attempt frequency, which for a particle is proportional to $\sqrt{U''(x)/m}$, for a GB has a more complex meaning that involves atomic vibrations both in the GB and in the grains. Since it enters the velocity expressions as a pre-exponential factor, it is less important than the jump barriers and for this discussion is assumed to be constant. Also, instead of fixing τ and computing the average velocity, we are interested in the average stress $\bar{\tau}$ or the average peak stress τ_c under a constant imposed velocity v. [Note that in the limit of large grains ($L\to\infty$) these stresses become almost identical.]

Figure 3 summarizes the stress-velocity relations expected from this model. In the region of small stresses and small velocities, we expect the linear dynamics according to Eq. (11), where $M(T)$ is often referred to as GB mobility.[32] The velocity range dominated by this "mobility regime" expands with temperature. The GB advances in a jittery manner in which many forward jumps are retracted. At large velocities and/or relatively low temperatures, the GB moves by predominantly (or exclusively) forward jumps. The stress-velocity relation is then strongly nonlinear and can be described by an equation similar to Eq. (13) with either the peak stress τ_c or the average stress $\bar{\tau}$.

The pre-exponential factor in Eq. (13) establishes the upper bounds of the velocity in the limit of $\tau_c\to\tau_c^0$, but in reality this equation loses its significance in this limit since the transition-state theory does not apply when the energy barrier is smaller than k_BT. Thus, this equation is valid as long as E_+ is significantly larger than k_BT but at the same time much smaller than E_0. Numerical estimates based on Eq. (5) indicate that even if E_+ is not much smaller than E_0, v is still an exponential function of stress but the power of $1-\tau_c/\tau_c^0$ is between 3/2 and 1.

IV. METHODOLOGY OF MD SIMULATIONS

In the rest of the paper, the dynamic relations based on the one-dimensional model will be tested against atomistic simulations. The MD simulations were performed with an embedded-atom method (EAM) potential[33] that accurately reproduces a variety of properties of Al, including the elastic constants, phonon frequencies, the intrinsic stacking fault energy, and others. Since the melting temperature of Al with this EAM potential was not calculated in the original paper,[33] this was done in this work using a method similar to Ref. 34. The melting temperature was found to be $T_m=1042$ K, which is approximately 10% higher than the experimental melting temperature of pure Al (933 K).[35] This implies that a comparison of our simulations with experiment should be based on homologous temperatures T/T_m.

To study GB motion, a simulation block with two grains separated by a flat GB was constructed. The block had an orthorhombic shape with periodic boundary conditions imposed in the directions parallel to the GB plane. To satisfy these conditions, the GB had to be a CSL boundary. Depending on the goal of a particular simulation, two types of boundary condition in the direction normal to the GB plane were applied. We refer to them as the fixed and free boundary conditions.

For the fixed boundary condition, the grains are sandwiched between two slabs parallel to the GB plane, in which the atoms are fixed in their perfect-lattice positions *relative to each other*. Each slab can be either fixed or allowed to move as a rigid body. All other atoms of the block are dynamic. The thickness of each slab is twice the cutoff radius of atomic interactions, which equals 0.126 nm for this potential. The thickness L of the dynamic region was chosen to be 12.2 nm, except in a few runs examining the size effect on the stress behavior as will be explained later.

The fixed boundary condition is convenient for applying a shear stress parallel to the boundary plane. To this end, the upper confining slap is moved with a constant velocity v in a chosen direction parallel to the GB plane, whereas the lower remains fixed. This boundary condition prohibits spontaneous rigid translation of the grains, although lattice regions adjacent to the GB can still translate relative to each other. Most of the simulations reported here were performed with $v=1$ m/s normal to the tilt axis. Some runs were also made with smaller velocities down to 0.1 m/s and up to 30 m/s in order to explore the velocity dependence of the shear stress.

In the free boundary condition, the previously fixed atoms of the upper slab are made dynamic, so that the upper grain now terminates at a free surface. The lower grain still remains attached to its fixed slab. Thus, the stress in the simulation block is always zero. This scheme allows free translations of the upper grain relative to the lower one. This boundary condition was applied to study spontaneous GB displacements in a coupled mode.

The MD simulations were implemented in the canonical (constant temperature, volume and number of atoms) ensemble using the ITAP Molecular Dynamics Program (IMD).[36] The MD integration time step was 0.2 fs and the total simulation time was 0.5–20 ns. Thermal expansion coefficients at different temperatures were determined by separate zero-pressure Monte Carlo simulations. Prior to the MD simulations, the block was uniformly expanded to include the effect of thermal expansion at the simulated temperature. That this procedure practically eliminates thermal stresses in the block was additionally confirmed by computing the average stress tensor without any applied loads and checking that all components were much smaller than typical stresses accompanying GB motion.

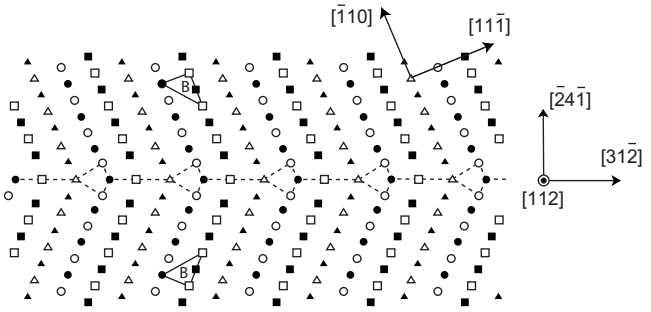

FIG. 4. Atomic structure of the $\Sigma 21$ $(\bar{2}4\bar{1})[112]$ (44.42°) GB at 0 K. The six different symbols represent atomic rows with different depth along the tilt axis [112] normal to the viewer. The order of the alternating (112) planes is as follows: solid triangle—solid square—solid circle—open triangle—open square—open circle. The open-circle layer is the deepest from the viewer. The structural units in the GB (kites) and in the grains (labeled B) are outlined. Note that their corners lie in different (112) planes.

The $\Sigma 21$ $(\bar{2}4\bar{1})$ [112] symmetrical tilt GB ($\theta=44.42°$) was chosen as a model.[37] Each grain had an approximately cubic shape and the entire block contained 24,190 atoms. The ground-state structure of the GB was determined by static minimization of the total potential energy with respect to local atomic displacements and relative translations of the grains. In addition, we checked that the ground state did not produce any long-range stresses in the grains.

The stress tensor $\hat{\boldsymbol{\sigma}}$ averaged over all dynamic atoms was computed using the standard virial expression and was constantly monitored during the simulations. The quantity of prime interest was the resolved shear stress τ parallel to the shear direction. During the simulations, the GB position was tracked using the centrosymmetry parameter P proposed in Ref. 38. The atomic layer parallel to the GB plane whose atoms had the largest value of P was identified with the boundary position.

V. SIMULATION RESULTS

A. Grain boundary structure and migration mechanism

The atomic structure of the GB at 0 K is shown in Fig. 4. The boundary consists of identical structural units with the shape of kites. Each row of such units running parallel to the tilt axis (and thus normal to the viewer) can be thought of as an edge dislocation with the Burgers vector $\mathbf{b}=[\bar{1}10]$. This Burgers vector was determined by a Burgers circuit construction using the upper grain as the reference lattice. This interpretation of the Burgers vector is consistent with the Cahn-Taylor work.[1] The GB energy calculated at 0 K is 0.443 J/m^2.

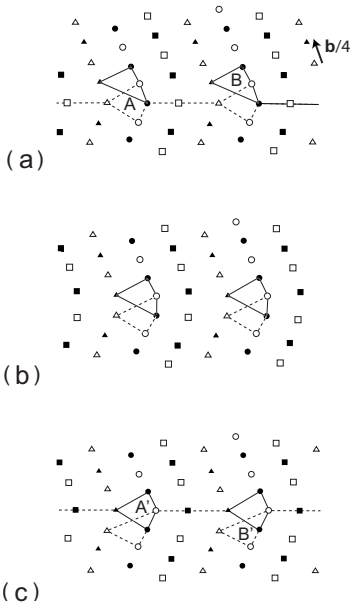

FIG. 5. Atomic mechanism for the coupled GB motion. (a) Initial state, (b) transition state, (c) final state. B is the lattice structural unit converting to the boundary unit A. A′ and B′ indicate the same structural units after the transformation.

When shear was applied by translating the upper fixed slab to the right, the GB was found to move up with an average velocity v_n proportional to the grain translation velocity v. Multiple snapshots stored during the MD simulations were analyzed to determine the atomic mechanism of the boundary motion, which is shown in Fig. 5. Consider the triangular structural unit B which belongs to the upper grain and is interlocked with the kite-shaped unit A. Note that B is a slightly distorted version of the perfect-lattice unit (cf. Fig. 4). Importantly, units A and B are topologically identical and can be transformed to each other by relatively small in-plane atomic displacements. At each step of boundary motion, each unit B changes its shape and transforms to a kite A′, whereas each unit A simultaneously transforms to a bulk unit B′ in the lower grain. Note that the latter is a mirror reflection of the B unit of the upper grain. As a result, the GB position shifts one step up while the upper grain translates to the right to accommodate the deformations of the units. This process can also be viewed as glide of the parallel array of GB dislocations along $(11\bar{1})$ planes of the upper grain.

This mechanism of GB motion was found to operate at temperatures 100 K and above. At 0 K, the applied shear stress produced rigid sliding of the upper grain without any GB displacement. This fact indicates that the critical stress of sliding at 0 K is smaller than the critical stress of coupled GB motion. Both stresses decrease with temperature and apparently a crossover occurs at some point below 100 K.

From the geometric theory of coupling,[4] it can be shown that the perfect coupling factor for this GB is $\beta = 2\tan(\theta/2) = (2/3)^{1/2} = 0.8165$.[39] The actual coupling factor was determined from the MD simulations as the ratio of the imposed v and the average GB migration velocity v_n. At temperatures up to 900 K $(0.86T_m)$, β was found to be practically independent of temperature and in good agreement with its geometrical value (Fig. 6), indicating that the coupling at these temperatures is nearly perfect. At 1000 K $(0.96T_m)$, a "dual behavior"[3] was observed in which the GB moved by sporadically switching back and forth between two coupling modes: the familiar one with $\beta \approx 0.817$ and a new mode that only appeared at high temperatures. The multiplicity of coupling modes is a separate topic that will be discussed elsewhere. In this paper we focus on coupled motion in one particular mode with $\beta = 0.8165$ and thus the temperature interval 100–900 K.

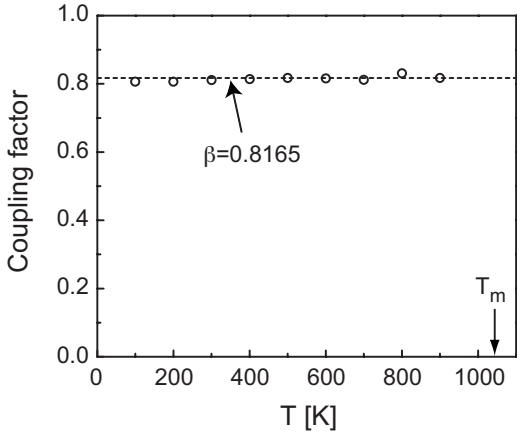

FIG. 6. Coupling factor β as a function of temperature obtained by MD simulations with $v = 1$ m/s. The dashed line shows the ideal geometric value of β. T_m is the bulk melting point of Al with this EAM potential.

The average step H of the GB motion obtained from the MD simulations is about 0.133 nm. To find the geometric value of H for this coupling mode, note in Fig. 5 that the GB dislocations glide along the $(11\bar{1})$ planes by increments of $\mathbf{b}/4 = [\bar{1}10]/4$. These planes make the angle $\theta/2$ with the GB normal. Thus, $H = (b/4)\cos(\theta/2) = a_0(3/28)^{1/2}$, which using the Al lattice parameter $a_0 = 0.405$ nm gives $H = 0.133$ nm in excellent agreement with our MD results. The average increment S of grain translations also accurately matches its geometric value $S = \beta H = 0.108$ nm.

B. Boundary dynamics: temperature dependence

Turning to the dynamics of the coupled GB motion, we will first discuss the effect of temperature under a fixed velocity $v = 1$ nm/s. Figure 7 indicates that the shear stress required for moving the GB decreases with temperature. Simultaneously, the character of the GB motion changes from incremental (stop-and-go) at relatively low temperatures to more stochastic at high temperatures. At low temperatures, stick-slip dynamics are clearly seen, with a saw-tooth behavior of the stress and a stepwise behavior of the GB position. Each peak of the stress correlates exactly with an increment of the GB motion: When a critical stress τ_c is reached, the boundary quickly moves a distance H up and stops, while the stress drops to a minimum value.

It was interesting to examine the grain-size effect on this stress behavior. To this end, some of the low-temperature simulations were repeated with $L = 6.4$, 9.6, 12.8, 16, and

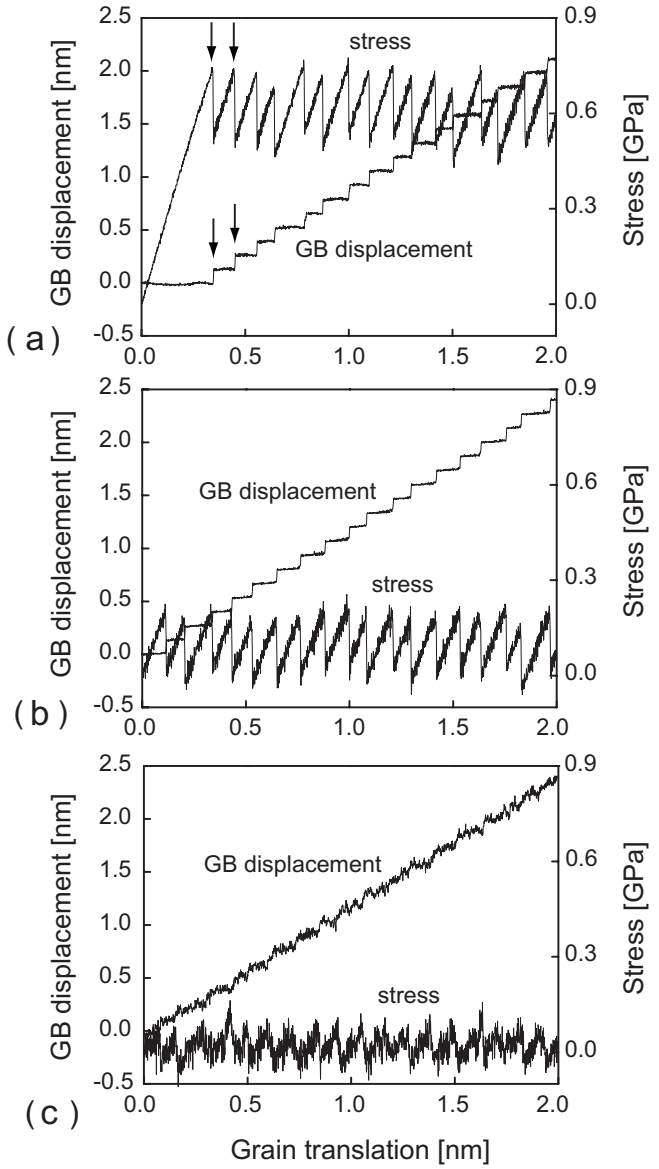

FIG. 7. GB displacement and shear stress at (a) 100 K, (b) 500 K, (c) 900 K and the imposed grain translation velocity $v=1$ m/s. The arrows indicate the correlation between the peaks of stress and the increments of the GB motion.

19.2 nm while keeping all other simulation conditions identical. The simulations confirm all trends predicted in Sec. II A. We find that the magnitude of the stress drop at each increment of the GB motion decreases with increasing L. At the same time, the peak stress hardly changes with L. As an example, Fig. 8 compares the stress behavior for two selected values of L. All subsequent simulations will be reported for just one grain size $L=12.2$ nm.

Returning to Fig. 7, we see that at 900 K ($0.86T_m$) the stepwise character of the GB motion is almost destroyed by thermal fluctuations and the saw-tooth behavior of the stress is much less pronounced than at low temperatures. Although the GB is still perfectly coupled (β matches its geometric value), the boundary dynamics have obviously undergone a transition.

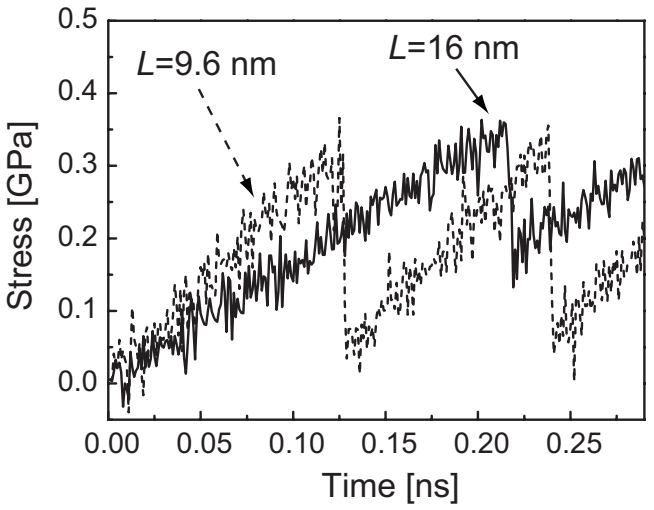

FIG. 8. Shear stress as a function of time in MD simulations of coupled GB motion with two different simulation block sizes L. In both cases, the temperature is 300 K and the imposed grain translation velocity is $v=1$ m/s. Note that the amount of the stress drop decreases with L whereas the peak stress remains the same.

To understand the nature of this dynamic transition, note that according to the stick-slip model discussed in Sec. III, $\log v$ is expected to be approximately linear in $(\tau_c^0-\tau_c)^{3/2}/k_BT$ as long as τ_c is close to its zero-Kelvin value τ_c^0. At a fixed v, the peak stress is therefore expected to be linear in $T^{2/3}$,

$$\tau_c = \tau_c^0 - BT^{2/3}, \tag{14}$$

where the constant B depends on the attempt frequency, the energy dissipation rate and other factors.

To test this relation, the peak stress at each temperature was averaged over 16–20 stick-slip events and plotted in Fig. 9 as a function of $T^{2/3}$. We also plot the stress $\bar{\tau}$ averaged over the entire time interval containing those stick-slip events. Although the absolute value of $\bar{\tau}$ depends on the grain size, this average stress should also be linear in $T^{2/3}$ in the stick-slip regime. We observe that both plots are indeed linear up to at least 500 K ($0.48T_m$). Together with the very clean saw-tooth behavior of the stress [cf. Figs. 7(a) and 7(b)], this linearity confirms that this temperature interval is indeed dominated by stick-slip dynamics.

Extrapolation of the linear relations to $T\to 0$ gives the "athermal" values $\tau_c^0=0.99$ GPa and $\bar{\tau}^0=0.87$ GPa. Using this τ_c^0, we find that the ratio τ_c/τ_c^0 varies between 0.74 at 100 K and 0.21 at 500 K. Recall that Eq. (14) was derived assuming that τ_c was close to τ_c^0 (Sec. III); it may not be accurate for such small values of τ_c/τ_c^0. Nevertheless, this equation does actually describe the MD results fairly well.

At temperatures 600 K ($0.57T_m$) and higher, both τ_c and $\bar{\tau}$ deviate from the straight lines and tend to level out. Combined with the noisy behavior of the stress and the GB position [Fig. 7(c)], these deviations indicate a transition to a dynamic regime different from stick-slip. We suggest that this regime is strongly driven Brownian dynamics.

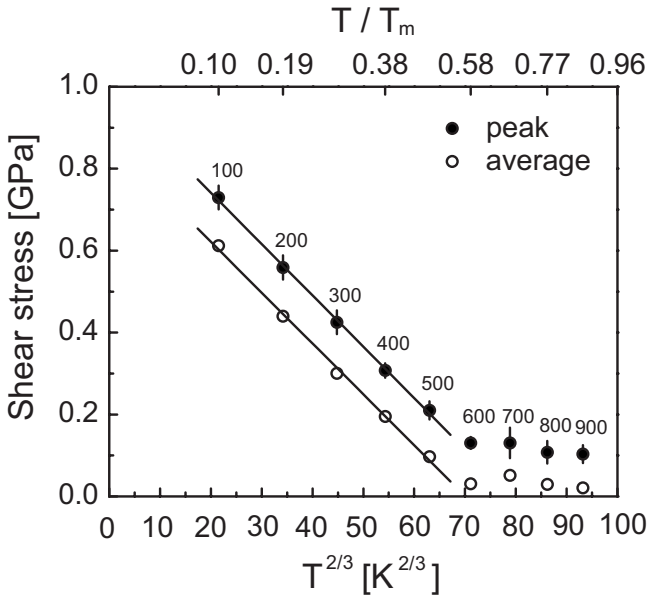

FIG. 9. Peak stress (solid circles) and average stress (open circles) as functions of temperature to the power 2/3 obtained by MD simulations with a constant velocity $v=1$ m/s. The numbers indicate the temperatures. The error bars represent the standard deviation of averaging over 16–20 stick-slip events. The lines show the linear correlation at temperatures 100–500 K.

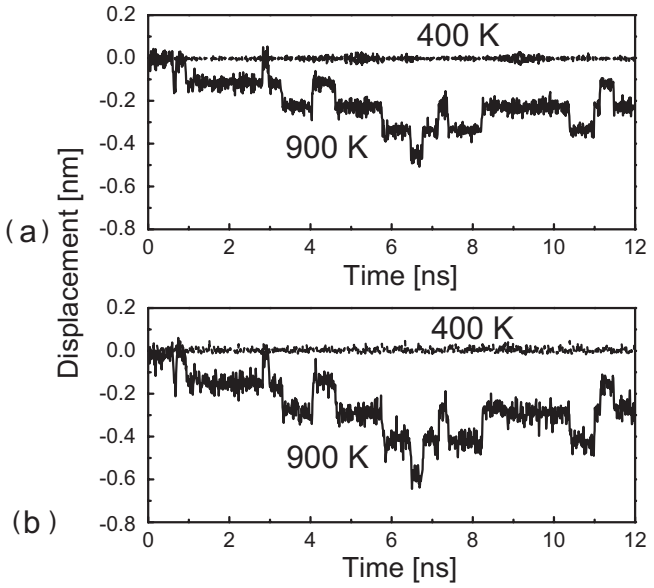

FIG. 10. Spontaneous coupled motion of the GB: (a) upper grain translation and (b) GB displacement and at 400 K and 900 K. The simulations were performed with the free boundary condition.

Indeed, while all GB jumps in the stick-slip mode occur in one direction (in our simulations, only upward), the driven Brownian regime is characterized by random jumps up and down, although the jumps up dominate. If the stress is completely removed, the GB must continue to jump up and down, implementing a random walk induced by continual thermal fluctuations. This prediction was tested by stress-free MD simulations at 900 K ($0.86T_m$) with the free boundary condition. The GB was indeed found to implement a random walk (Fig. 10); in fact, given enough time it could wander quite far away from its initial position. These spontaneous GB movements were accompanied by simultaneous translations of the upper grain due to the coupling effect. By contrast, at 400 K ($0.38T_m$) (a temperature inside the stick-slip range) the boundary did not make any spontaneous movements.

Figure 10 demonstrates that there is a close correlation between the boundary displacements and the upper grain translations during the random walk at 900 K. To quantify this correlation, we plot in Fig. 11 the GB displacement relative to the initial position versus the translation of the center of mass of the upper grain perpendicular to the tilt axis. An excellent linear correlation is apparent, with the slope of 0.843 which is close to the geometric coupling factor 0.8165. These observations are consistent with the fact[4] that the coupling factor does not depend on whether the GB motion is induced by thermal fluctuations or driven by an applied stress.

When a stress is applied at 900 K, it biases the existing random jumps of the boundary and drives it *on average* upward. Attempts were made to directly observe backward GB jumps during the stress-driven simulations at high temperatures. It should be noted that in such simulations, the fixed boundary condition constrains spontaneous rigid translations of the grains, although local translations near the GB are still possible. Since such local translations come at the expense of elastic deformation of the surrounding lattice regions, the spontaneous GB movements cannot be as extensive as they are with the free boundary condition. Nevertheless, they are expected to occur at high enough temperatures.

Unfortunately, we were not able to see backward GB jumps in the stress-driven simulations. Presumably, the bias imposed by the stress was too strong and made the backward jumps rare events. Given also the significant distortions of the GB structure produced by the stress, the few backward jumps that still happened were not detected by our visualization method. One way to reveal them would be to drastically reduce the GB velocity using accelerated MD methods,[17] but

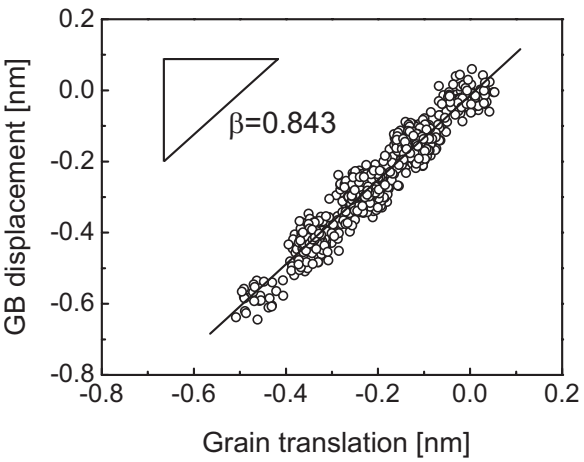

FIG. 11. Grain boundary displacement as a function of GB translation during spontaneous coupled GB motion at 900 K. The slope of the correlation line gives an estimate of the correlation factor β.

this was not pursued in this work. We emphasize that under real conditions, the GB velocities encountered in experiments on bicrystals or during recrystallization and growth in polycrystalline materials are orders of magnitude smaller than in our simulations.[32] At such small velocities, spontaneous GB displacements coupled to lattice translations can occur much more readily. Thus, in real materials at high temperatures, the coupled GB motion is likely to occur by driven Brownian motion.

C. Boundary dynamics: velocity dependence

The low- and high-temperature regimes of the GB motion were also studied by fixing a temperature and varying the imposed grain translation velocity. Two different temperatures were tested, 400 K ($0.38T_m$) and 900 K ($0.86T_m$), each with velocities ranging from 0.1 up to 30 m/s. The results were analyzed in terms of velocity-stress relations at these temperatures. The average stress $\bar{\tau}$ was used since it could be computed more accurately than τ_c.[40]

At $T=400$ K, the GB remained coupled with $\beta \approx 0.817$ and exhibited a saw-tooth behavior of the stress over the entire velocity range. The velocity-stress relation obtained is highly nonlinear as shown in Fig. 12(a). At low stresses, v increases with $\bar{\tau}$ extremely slowly until ~0.18 GPa. Although we expect v to become a linear function of $\bar{\tau}$ at small enough velocities, this linear regime was not actually revealed at this temperature. Implementing this regime would require reducing v significantly below 0.1 m/s. To reach such small velocities, the MD time had to be longer than 50–100 ns (the time to move the GB over at least a few nanometers). Implementing this regime was beyond our computational resources.

Above ~0.18 GPa, the growth of v with $\bar{\tau}$ rapidly accelerates and by $\bar{\tau} \approx 0.20$ GPa (which corresponds to $v \approx 5$ m/s) the plot becomes almost vertical. The log v versus $\bar{\tau}$ plot shown in Fig. 12(b) indicates that at $v \leq 5$ m/s the rapid growth of v can be described as approximately exponential in stress. Analysis shows that it can also be described as exponential with respect to $(\bar{\tau}^0 - \bar{\tau})^{3/2}$ within the scatter of the points. Although the limited statistics do not permit us to distinguish between the powers of 1 and 3/2, the important point is that the growth of v is exponentially fast in agreement with the analysis in Sec. III.

The departure from the exponential growth at higher velocities ($v > 10$ m/s) is explained by the effect of dynamic correlations between the GB jumps. At such high velocities, the energy dissipation rate cannot catch up with the elastic strain energy release at each step of the boundary motion. The undamped energy, existing in the form of sound waves bouncing back and forth between the two fixed regions, assists the GB in overcoming the next activation barrier. This produces a decrease in the stress required for moving the GB in comparison with the low-velocity regime in which the GB completely thermalizes after each jump. In the strongly underdamped regime observed at high velocities, the transition-state theory does not apply and the GB motion does not have to follow the exponential relations derived in Sec. III based on this theory. At even higher velocities, the curve could turn over and produce a regime in which the velocity decreases with increasing stress. This regime was indeed found in the recent MD study of a copper GB.[17] We emphasize that, although this effect is generic, the velocity range in which it occurs depends on the dissipation mechanisms, temperature, grain size and many other factors.

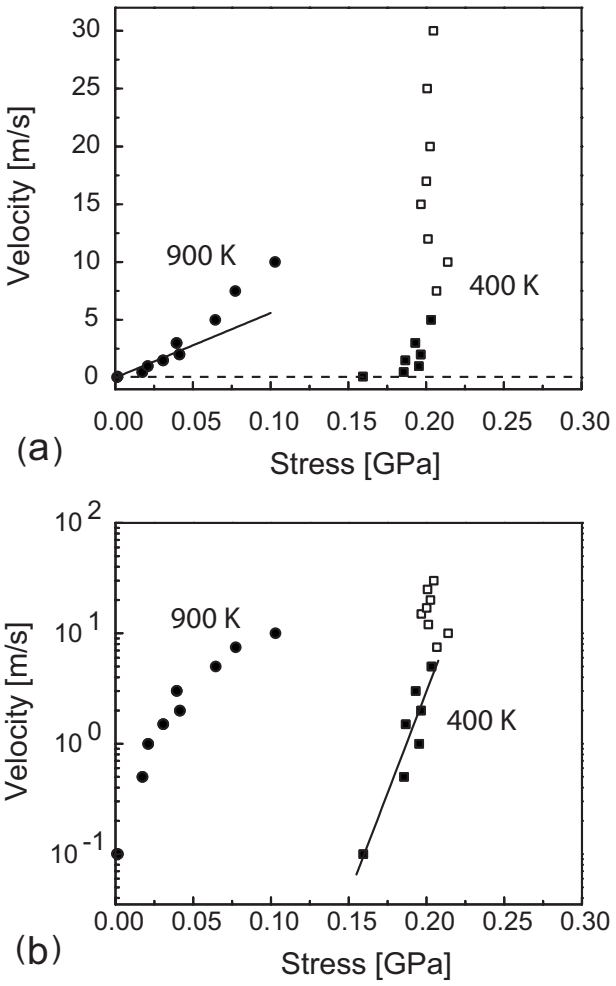

FIG. 12. The GB velocity (a) and its logarithm (b) as functions of the average shear stress at temperatures 400 and 900 K. The open squares indicate velocities at which multiple jumps are observed. The dashed line in (a) indicates the zero velocity; the solid lines are linear fits.

A convincing proof of the existence of the dynamic correlations is the observation of double jumps of the GB at $v > 10$ m/s. In such events, illustrated in Fig. 13, the boundary makes a jump by the double amount $2H$ and the stress drops to a lower level than it does after a single jump. This happens because the elastic strain energy released after the first jump is large enough to immediately produce another jump. In fact, at velocities higher than 15 m/s we saw triple and even higher multiple jumps. There is an interesting analogy between such multiple jumps in coupled GB motion and the multiple slip events found recently in atomic-scale friction experiments.[22,41,42]

At the temperature of 900 K, the GB motion remains perfectly coupled at velocities up to ~10 m/s. Above 10 m/s, the coupled motion begins to be interrupted by occa-

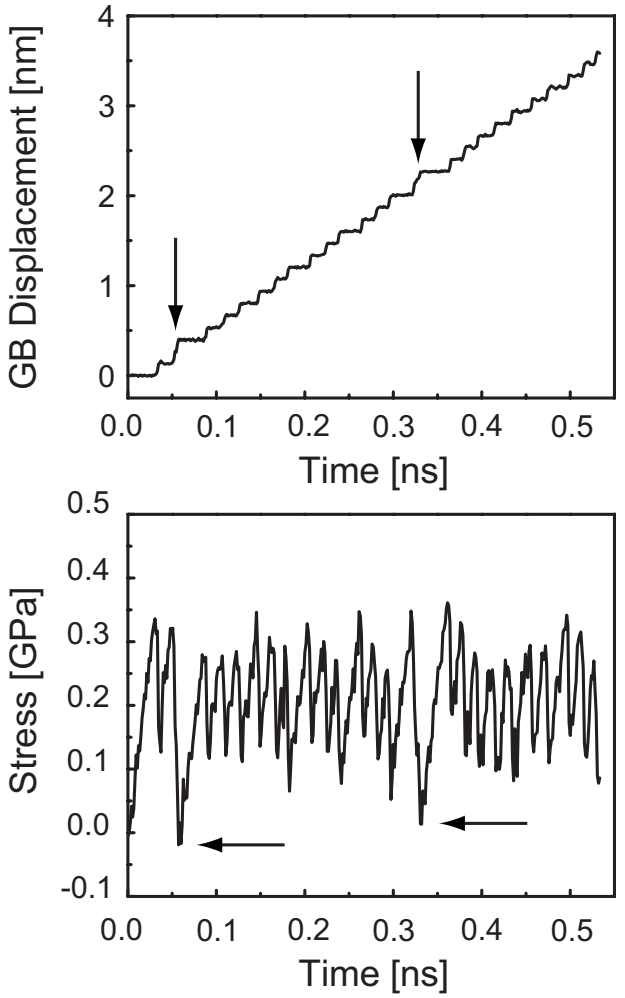

FIG. 13. Stick-slip GB motion at 400 K and $v=7.5$ m/s. The double jumps are indicated by arrows.

sional sliding events as indicated in Fig. 14 (the sliding events are manifested by nearly horizontal parts of the curve). Between the sliding events, the GB continues to move in the coupling mode with $\beta \approx 0.8165$. As v increases further, the frequency of the sliding events also increases until at $v \approx 30$ m/s sliding becomes the dominant response of the boundary to the applied shear stress. Although the velocity dependence of sliding was not studied in this work, these results suggest that the stress required for sliding is less sensitive to v than $\bar{\tau}$ is, producing a crossover of the two stresses at about 0.15 GPa (corresponding to $v \approx 10$ m/s) at this temperature.

In the velocity range of perfect coupling at 900 K, the velocity-stress relation is overall nonlinear but it does exhibit a nearly linear part below $v \approx 3$ m/s. This linear regime is well-consistent with the driven Brownian character of the GB motion at this temperature (Sec. V B). The nonlinear behavior exhibited at higher velocities marks a transition to the stick-slip dynamics, characterized by a rapid (roughly, exponential) increase in velocity with stress. Overall, the stress-velocity relations found by the MD simulations [Fig. 12(a)] compare well with predictions of the one-dimensional model discussed in Sec. III (Fig. 3).

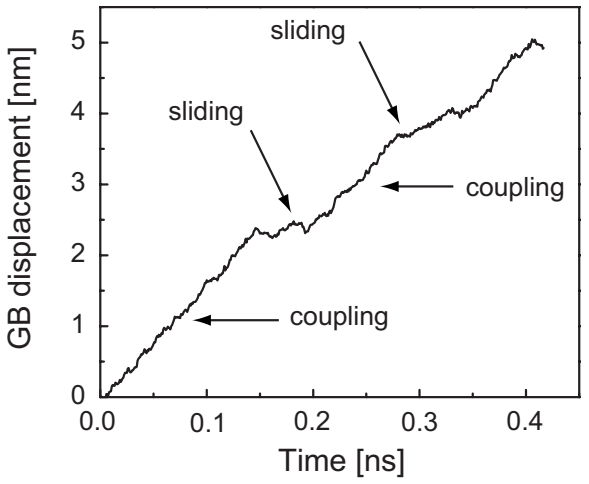

FIG. 14. Coupled GB motion interrupted by sliding events at 900 K. The imposed grain translation velocity is 12 m/s.

VI. CONCLUSIONS

We have analyzed possible dynamic regimes of coupled GB motion using two different approaches. The one-dimensional model discussed in Sec. III is a crude analog of the complex multidimensional process taking place during the GB motion, but it can predict simple analytical relations between the GB velocity, stress, and temperature. The MD simulations bring us closer to reality, but the results are only numerical and the simulated conditions are subject to the time and length-scale limitations of the method. As a result, only a limited area of the parameter space can be explored by MD. Despite these differences, the two methods give qualitatively consistent results that can be summarized as follows:

At low temperatures and/or high migration velocities, a coupled GB exhibits stick-slip behavior characterized by incremental (stop-and-go) motion and a saw-tooth time dependence of the stress. The average velocity increases with the average stress in a highly nonlinear manner, close to exponential. The GB makes jumps only forward and stops as soon as the applied stress is removed. As temperature rises and/or the velocity slows down, the GB begins to make occasional reverse jumps and eventually switches from the stick-slip regime to driven Brownian motion. The stress-velocity relation approaches linear, with a coefficient which is often called "mobility."[32] When the stress is completely removed, the GB continues to implement random walk due to thermal fluctuations. We emphasize that throughout all these dynamic changes, the boundary motion still remains perfectly coupled, with the ratio of the normal GB velocity to the grain translation velocity being a geometric constant. The perfect coupling remains even for the stress-free random walk at high temperatures.

Most of the GB migration experiments, as well as atomistic simulations, reported in the literature (e.g., Refs. 7, 8, and 43–45), have been conducted at relatively high temperatures. They typically display a linear stress-velocity relation indicative of Brownian dynamics. There are cases, however, when nonlinear dynamics were also observed,[45–47] but their physical origin and atomic mechanisms were not investigated.

In the future, the one-dimensional model of Sec. III can be examined in greater detail by including the effects of inertia and underdamping, perhaps in a manner similar to Refs. 31 and 48. This might help better understand the double jumps and other interesting dynamic effects observed at high velocities. Another model that we are exploring is the driven Frenkel-Kontorova[49] model. We will also examine the grain-size effect on GB dynamics, particularly the effect of the GB area. The latter could be important since the GB dimensions in comparison with the critical nucleation size of disconnection loops[4] responsible for the coupled motion can affect the dynamics regimes.

ACKNOWLEDGMENTS

We would like to thank J. W. Cahn and D. A. Molodov for helpful discussions. We are grateful to the Center for Theoretical and Computational Materials Science of the National Institute of Standards and Technology for making their computational cluster available for this work. This work was supported by the U.S. Department of Energy (Office of Basic Energy Sciences, Division of Materials Sciences). We acknowledge useful discussions facilitated through coordination meetings sponsored by the DOE-BES Computational Materials Science Network (CMSN) program.

*vivanov@gmu.edu
†ymishin@gmu.edu

[1] J. W. Cahn and J. E. Taylor, Acta Mater. **52**, 4887 (2004).
[2] A. Suzuki and Y. Mishin, Mater. Sci. Forum **502**, 157 (2005).
[3] J. W. Cahn, Y. Mishin, and A. Suzuki, Philos. Mag. **86**, 3965 (2006).
[4] J. W. Cahn, Y. Mishin, and A. Suzuki, Acta Mater. **54**, 4953 (2006).
[5] If the crystal is elastically anisotropic and the boundary asymmetric, the shear stress can create a volume driving force due to the difference between the elastic strain energy densities in the grains. This driving force is quadratic in the stress and is not considered in this paper. The interaction of coupled GBs with stresses is a first-order effect, in which the driving force is linear in stress.
[6] S. G. Srinivasan and J. W. Cahn, in *Science and Technology of Interfaces*, edited by S. Ankem, C. S. Pande, I. Ovidko, and R. Ranganathan (TMS, Seattle, 2002), pp. 3–14.
[7] D. Molodov, A. Ivanov, and G. Gottstein, Acta Mater. **55**, 1843 (2007).
[8] D. Molodov, T. Gorkaya, and G. Gottstein, Mater. Sci. Forum **558-559**, 927 (2007).
[9] M. Winning, G. Gottstein, and L. S. Shvindlerman, Acta Mater. **49**, 211 (2001).
[10] M. Winning, G. Gottstein, and L. S. Shvindlerman, Acta Mater. **50**, 353 (2002).
[11] M. Winning and A. D. Rollett, Acta Mater. **53**, 2901 (2005).
[12] M. Winning, Philos. Mag. **87**, 5017 (2007).
[13] H. Yoshida, K. Yokoyama, N. Shibata, and Y. I. A. T. Sakuma, Acta Mater. **52**, 2349 (2004).
[14] J. Monk, B. Hyde, and D. Farkas, J. Mater. Sci. **41**, 7741 (2006).
[15] K. J. Hemker and W. N. Sharpe, Annu. Rev. Mater. Res. **37**, 93 (2007).
[16] T. Zhu, J. Li, A. Samanta, H. G. Kim, and S. Suresh, Proc. Natl. Acad. Sci. U.S.A. **104**, 3031 (2007).
[17] Y. Mishin, A. Suzuki, B. P. Uberuaga, and A. F. Voter, Phys. Rev. B **75**, 224101 (2007).
[18] D. A. Molodov (private communication).
[19] A. P. Sutton and R. W. Balluffi, *Interfaces in Crystalline Materials* (Clarendon, Oxford, 1995).
[20] The superscript 0 in τ_c^0 is a reminder that this critical stress refers to zero temperature.
[21] It is implied that the elastic strain energy released at each increment of the GB motion is immediately dissipated and the temperature comes back to 0 K.
[22] C. M. Mate, G. M. McClelland, R. Erlandsson, and S. Chiang, Phys. Rev. Lett. **59**, 1942 (1987).
[23] E. Gnecco, R. Bennewitz, T. Gyalog, C. Loppacher, M. Bammerlin, E. Meyer, and H.-J. Güntherodt, Phys. Rev. Lett. **84**, 1172 (2000).
[24] E. Gnecco, R. Bennewitz, T. Gyalog, and E. Meyer, J. Phys.: Condens. Matter **13**, R619 (2001).
[25] A. Socoliuc, E. Gnecco, S. Maier, O. Pfeiffer, A. Baratoff, R. Bennewitz, and E. Meyer, Science **313**, 207 (2006).
[26] D. Tomanek, W. Zhong, and H. Thomas, Europhys. Lett. **15**, 887 (1991).
[27] K. Johnson and J. Woodhouse, Tribol. Lett. **5**, 155 (1998).
[28] One could attempt to approximate the force-reduced barrier by $E_+ \approx E_0 - \tau a/2$ since in the absence of forces the energy maximum occurs at $x=a/2$. This barrier would go through zero as a linear function of τ, which is incorrect. The linear approximation of E_+ is valid only when τ is small but fails when τ is large enough to eliminate the barrier. The reason is that τ also shifts the positions of the equilibrium point (x_0) and the maximum (x_1), bringing them closer to each other until they merge as the barrier tends to zero. This merger of x_0 and x_1 makes the decrease of E_+ with τ slower than linear, which is reflected by the power of 3/2.
[29] A. Garg, Phys. Rev. B **51**, 15592 (1995).
[30] Y. Sang, M. Dube, and M. Grant, Phys. Rev. Lett. **87**, 174301 (2001).
[31] P. Reimann and M. Evstigneev, New J. Phys. **7**, 25 (2005).
[32] G. Gottstein and L. S. Shvindlerman, *Grain Boundary Migration in Metals* (CRC, Bota Raton, 1999).
[33] Y. Mishin, D. Farkas, M. J. Mehl, and D. A. Papaconstantopoulos, Phys. Rev. B **59**, 3393 (1999).
[34] J. Morris and X. Song, J. Chem. Phys. **116**, 9352 (2002).
[35] *Smithells Metals Reference Book*, 8th ed., edited by W. Gale and T. Totemeier (Elsevier, New York/Butterworth, Washington, DC/Heinemann, London, 2004).
[36] J. Stadler, R. Mikulla, and H. R. Trebin, Int. J. Mod. Phys. C **8**, 1131 (1997).
[37] In this paper, all crystallographic indices are given relative to the lattice of the upper grain.
[38] C. L. Kelchner, S. J. Plimpton, and J. C. Hamilton, Phys. Rev. B

58, 11085 (1998).

[39] It can be shown that for this GB $\sin(\theta/2)=(1/7)^{1/2}$, $\cos(\theta/2)=(6/7)^{1/2}$ and thus $2\tan(\theta/2)=(2/3)^{1/2}$.

[40] At high temperatures and/or large velocities, the peak stress becomes noisy and in some cases cannot be even resolved.

[41] Y. Hoshi, T. Kawagishi, and H. Kawakatsu, Jpn. J. Appl. Phys., Part 1 **39**, 3804 (2000).

[42] S. N. Medyanik, W. K. Liu, I. H. Sung, and R. W. Carpick, Phys. Rev. Lett. **97**, 136106 (2006).

[43] D. A. Molodov, G. Gottstein, F. Heringhaus, and L. S. Shvindlerman, Acta Mater. **46**, 5627 (1998).

[44] V. Ivanov, D. Molodov, L. Shvindlerman, and G. Gottstein, Acta Mater. **52**, 969 (2004).

[45] B. Schönfelder, D. Wolf, S. R. Phillpot, and M. Furtkamp, Interface Sci. **5**, 245 (1997).

[46] H. Zhang, M. I. Mendelev, and D. J. Srolovitz, Acta Mater. **52**, 2569 (2004).

[47] B. Schönfelder, Ph.D. thesis, IMM, RWTH-University, 2004.

[48] M. Evstigneev and P. Reimann, Phys. Rev. B **73**, 113401 (2006).

[49] O. M. Brun and Y. S. Kivshar, *The Frenkel-Kontorova Model: Concepts, Methods, and Applications, Theoretical and Mathematical Physics* (Springer-Verlag, Berlin, 2004).